

Shock wave assisted intracellular delivery of antibiotics against bone infection with *Staphylococcus aureus* via P2X7 receptors[☆]

Jiangbi Li^{a,b}, Haixia Li^c, Songqi Bi^a, Yang Sun^a, Feng Gu^d, Tiecheng Yu^{a,1,*}

^a Department of Orthopedics, Orthopaedic Center, The First Hospital of Jilin University, Changchun, Jilin, China

^b Department of Orthopaedics, Yunnan Cancer Hospital, The Third Affiliated Hospital of Kunming Medical University, Kunming, Yunnan, China

^c Department of Neurology, The Affiliated Hospital of Kunming University of Science and Technology, the First People's Hospital of Yunnan Province, Kunming, Yunnan, China

^d Department of Orthopedics, The Second Hospital of Jilin University, Changchun, Jilin, China

ARTICLE INFO

Keywords:

Chronic osteomyelitis

Shock wave

Cell membrane permeability

Osteoblasts

P2X7 receptors

ABSTRACT

Background: Treatment of chronic osteomyelitis (bone infection) remains a clinical challenge; in particular, it requires enhanced delivery of antibiotic drugs for the treatment of intracellular *Staphylococcus aureus* (*S. aureus*), which prevents infection recurrence and resistance. Previous studies have found that noninvasive shock waves used to treat musculoskeletal diseases can alter cell permeability, however, it is unclear whether shock waves alter cell membrane permeability in chronic osteomyelitis. Furthermore, it remains unknown whether such changes in permeability promote the entry of antibiotics into osteoblasts to exert antibacterial effects.

Methods: In our study, trypan blue staining was used to determine the shock wave parameters that had no obvious damage to the osteoblast model; the effect of shocks waves on the cell membrane permeability of osteoblast model was detected by BODIPY®FL vancomycin; high performance liquid chromatography-mass spectrometry (HPLC-MS) was used to detect the effect of shock wave on the entry of antibiotics into the osteoblast model; plate colony counting method was used to detect the clearance effect of shock wave assisted antibiotics on *S. aureus* in the osteoblast model. To explore the mechanism, the effect of different pulses of shock waves on *S. aureus* was examined by plate colony counting method, besides, P2X7 receptor in osteoblast was detected by immunofluorescence and the extracellular ATP levels was detected. Furthermore, the effect of P2X7 receptor antagonists KN-62 or A740003 on the intracellular antibacterial activity of shock-assisted antibiotics was observed. Then, we used *S. aureus* to establish a rat model of chronic tibial osteomyelitis and investigated the efficacy and safety of shock-wave assisted antibiotics in the treatment of chronic osteomyelitis in rats.

Results: The viability of the osteoblast models of intracellular *S. aureus* infection was not significantly affected by the application of up to 400 shock wave pulses at 0.21 mJ/mm². Surprisingly, the delivery of BODIPY®FL vancomycin to osteoblast model cells was markedly enhanced by this shock wave treatment. Furthermore, the shock wave therapy increased the delivery of hydrophilic antibiotics (vancomycin and cefuroxime sodium), but not lipophilic antibiotics (rifampicin and levofloxacin), which improved the intracellular antibacterial effect. Afterwards, we discovered that shock wave treatment increased the extracellular concentration of ATP (the P2X7 receptor activator), while KN-62 or A740003, a P2X7 receptor inhibitor, decreased intracellular antibacterial activity. We then found that 0.1 mL of 1×10^{11} CFU/mL ATCC25923 *S. aureus* was suitable for modeling chronic osteomyelitis in rats. Besides, the shock wave-assisted vancomycin treatment with the strongest antibacterial and osteogenic effects among the tested treatments was confirmed in vivo by imaging examination, microbiological cultures, and histopathology, with favorable safety.

[☆] The translational potential of this article: This study attempts to explore a novel intracellular anti-infection method, which is rarely reported in previous studies. In addition, through in vivo and in vitro experiments, the effectiveness of shock wave assisted antibiotics in the treatment of *S. aureus* infection in osteoblasts was proved, which provides a new treatment strategy for the treatment of chronic osteomyelitis.

* Corresponding author.

E-mail addresses: lijb312@163.com (J. Li), haixiali6677@163.com (H. Li), bisq7018@163.com (S. Bi), sunyang.rocket@outlook.com (Y. Sun), gufengjlu@163.com (F. Gu), yutc@jlu.edu.cn (T. Yu).

¹ Present address: No. 1 Xinmin Street, Changchun City, Jilin Province, China

<https://doi.org/10.1016/j.jot.2023.10.006>

Received 4 August 2023; Accepted 20 October 2023

2214-031X/© 2023 The Authors. Published by Elsevier B.V. on behalf of Chinese Speaking Orthopaedic Society. This is an open access article under the CC BY-NC-ND license (<http://creativecommons.org/licenses/by-nc-nd/4.0/>).

Conclusions: Our results suggest that shock waves can promote the entry of antibiotics into osteoblasts for antibacteria by changing the cell membrane permeability in a P2X7 receptor-dependent manner. Besides, considering antibacterial and osteogenic efficiency and a high degree of safety in rat osteomyelitis model, shock wave-assisted vancomycin treatment may thus represent a possible adjuvant therapy for chronic osteomyelitis.

1. Introduction

Osteomyelitis is a bacterial infectious disease of bone tissue accompanied by bone destruction and sepsis, which are caused by infectious microorganisms after trauma, bone surgery, diabetic foot, or joint replacement [1,2]. It remains a substantial healthcare burden with a prevalence of ~22 cases per 100,000 individuals per year in the United States, and its incidence has been increasing over time, particularly in the elderly and individuals with diabetes [3]. Although many organisms can cause skeletal infections, *Staphylococcus aureus* remains the most prevalent and dangerous causal pathogen [4]. Local and systemic infection control is critical for the treatment of adult osteomyelitis. Surgical debridement and a high parenteral dose of systemic antibiotics are required in most adult patients with osteomyelitis [2]. However,

such standard therapies not only fail at a rate of up to 30 % but also result in tissue defects, drug resistance, and organ toxicity [5].

S. aureus infects bone tissue and internalizes into osteoblasts, evading the body’s immune response and antibiotics through vesicle escape and the formation of small colony variants (SCVs). As a result, *S. aureus* can survive for a long time after its internalization into osteoblasts [6,7]. In fact, most antibiotics are ineffective against intracellular pathogens due to their low retention inside the cells (i.e., macrolides or fluoroquinolones) [8] or poor entry into the cells (i.e., β-lactams or aminoglycosides) [9,10]. Vancomycin, in particular, is a last-resort antibiotic against methicillin-resistant *S. aureus* (MRSA), however it cannot eradicate intracellular MRSA due to its limited uptake by infected host cells [11]. The intracellular location of these bacteria offers protection from the host’s immune response, and can result in cell alterations and

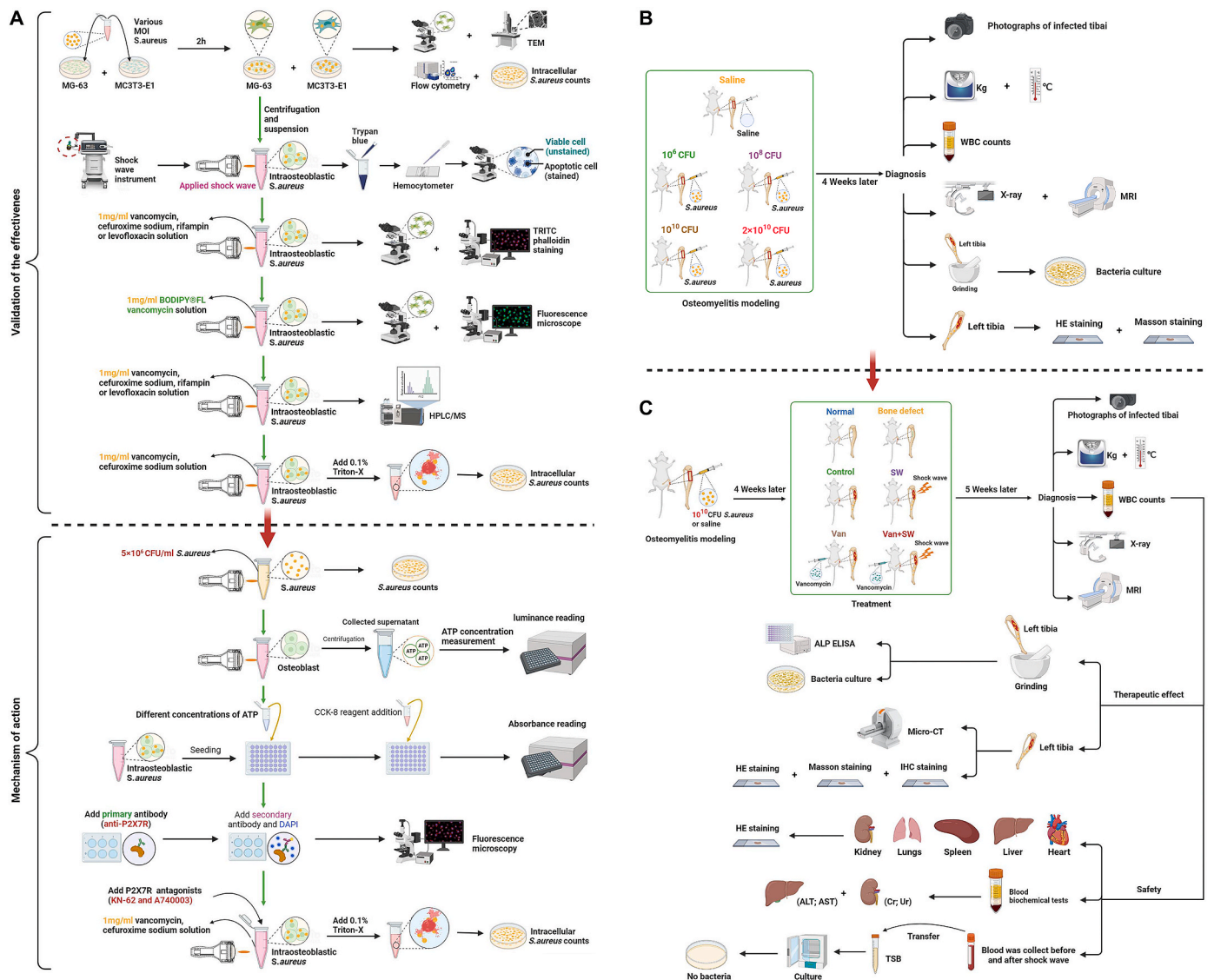


Fig. 1. Experimental design and protocol (A) Effectiveness and mechanism of shock wave-assisted antibiotics in the treatment of intraosteoblastic *S. aureus* (B) Establishment of chronic osteomyelitis experiment in rats (C) Shock wave-assisted vancomycin treatment for chronic osteomyelitis in rats.

bacterial resistance if exposed to subtherapeutic concentrations of antibiotics [12]. In addition, the proliferation and differentiation abilities of osteoblasts with internalized *S. aureus* are weakened, leading to a reduction in bone tissue formation. In addition, intracellular *S. aureus* can cause apoptosis and necrosis of osteoblasts. After the release of “hidden” *S. aureus*, it can infect other osteoblasts and cause repeated infection of bone tissue, leading to chronic osteomyelitis [13,14]. Although antibiotic-loaded nanoparticles [15], antimicrobial peptides [16], or phagotherapy [17] have been experimentally shown to have suitable efficacy in the treatment of intracellular bacteria, their clinical application in treating osteomyelitis patients is still a long way off. Therefore, it is extremely desirable to develop novel antibiotics and effective strategies to treat osteomyelitis.

Extracorporeal shock wave therapy (ESWT) is a noninvasive treatment developed on the basis of shock wave lithotripsy, which has become an important method for the treatment of urinary calculi [18, 19]. Furthermore, the biological effects of ESWT have been reported, including tissue regeneration, wound healing, angiogenesis, bone remodeling, anti-inflammation, anti-apoptosis, and nerve regeneration [20,21]. ESWT has also been used to treat musculoskeletal diseases [21], repair acute and chronic motor system injury diseases [22], acute and chronic wound healing, diabetic foot ulcers, ischemic cardiomyopathy, and erectile dysfunction [23]. Shock waves (SWs) can also increase the permeability of the cell membrane, allowing substances that do not easily pass through cell membranes, such as calcein and fluorescent yellow, to enter the cells [24,25]. Hydrophilic antibiotics have difficulty entering the cell through the hydrophobic membrane, so that intracellular bacteria can escape the killing effect of antibiotics. Therefore, we speculate that shock waves can effectively treat intracellular infection by increasing the permeability of the cell membrane and promoting the entry of antibiotics into osteoblasts.

In this study, we report a novel intracellular anti-infection method for the treatment of *S. aureus*-infected osteomyelitis (Fig. 1). We first conducted in vitro experiments to determine the effectiveness and mechanisms of shock wave-assisted antibiotic delivery against intracellular *S. aureus*. We found that shock waves could increase the membrane permeability of osteoblasts and enhance the intracellular antibacterial effect by promoting the delivery of vancomycin and cefuroxime sodium by the cells, and the mechanism was related to the ATP/P2X7 receptor pathway. Next, we investigated the effectiveness of shock wave-assisted antibiotics in the treatment of chronic osteomyelitis in rats, and we found that shock wave-assisted vancomycin treatment has significant anti-infective and osteogenic effects and could quickly improve liver and kidney function in chronic osteomyelitis model rats, with no toxic side effects on the organism and suitable safety. Hence, this work provides a feasible strategy for the effective treatment of chronic osteomyelitis.

2. Materials and methods

2.1. Materials

MG-63 and MC3T3-E1 cells were purchased from Shanghai Cell Bank of Chinese Academy of Sciences (Shanghai, China); *S. aureus* (ATCC 25923) was obtained from School of Basic Medical Science, Jilin University; Tryptone soybean broth (TSB) and brain heart infusion agar (BHIA) were purchased from Haibo Biotechnology Co., Ltd (Qingdao, China); Lysostaphin were purchased from Biorab Technology Co., Ltd (Beijing, China); Triton X-100 were purchased from Biofrox (Germany); BODIPY®FL vancomycin was purchased from Thermo Fisher Scientific (Waltham, MA, USA); vancomycin, cefuroxime sodium, rifampin or levofloxacin was purchased from Yuanye Bio-Technology Co., Ltd (Shanghai, China); Trypan blue staining solution was purchased from Dingguo Changsheng Biotechnology Co., Ltd; Rhodamine-labeled phalloidin was purchased from Solarbio Science & Technology Co.,Ltd (Beijing, China); The CCK-8 reagent, PBS, Trypsin–EDTA digest solution,

and triphosadenine (ATP) was purchased from New Cell &Molecular Biotech Co., Ltd (Suzhou, China); CellTiter-Lumi™ Plus Luminescent Cell Viability Assay Kit, DAPI staining solution and Alexa Fluor 555-labeled Donkey Anti-Rabbit IgG (H + L) was purchased from Beyotime Biotech. Inc (Shanghai, China); P2X7 receptor antibody was purchased from Alomone labs (Jerusalem, Israel); KN-62 and A740003 were purchased from MedChemExpress (New Jersey, USA); Male Wistar rats (12-weeks-old) were purchased from the Animal Experiment Center of Jilin University (China), and a rat ALP ELISA kit was purchased from Sen-BeiJia Biological Technology Co., Ltd (Nanjing, China).

2.2. Validation of the effectiveness of shock wave-assisted antibiotics in the treatment of intraosteoblastic *S. aureus*

2.2.1. Cell and bacterial culture

At 37 °C in a 5 % CO₂ humidified atmosphere, MG-63 cells were cultured in high-glucose DMEM (Hyclone) medium supplemented with 10 % fetal bovine serum (FBS), and MC3T3-E1 cells were cultured in α -MEM (Hyclone) medium supplemented with 10 % FBS. *S. aureus* (ATCC 25923) was cultured in TSB. At the time of osteoblast infection, the absorbance at 600 nm (A600) of the bacterial suspension was adjusted to 0.5 (corresponding to 10⁹ bacteria).

2.2.2. Establishment of intracellular infection of *S. aureus* in (human and mouse) osteoblast models

An intracellular infection assay was performed using a modified method similar to that developed by Hamza et al. [26].

The intracellular infection assay is described in [Supplementary Methods 1.1](#).

2.2.3. Extracorporeal shock wave exposure

The determination of the optimal experimental conditions for shock waves is described in [Supplementary Methods 1.2](#).

2.2.4. Effect of shock waves on osteoblasts in antibiotic solution

The effect of shock waves on osteoblasts in antibiotic solution is described in [Supplementary Methods 1.3](#).

2.2.5. Effect of shock waves on cell membrane permeability in intracellular *S. aureus* infection models

Infected osteoblast models were developed as described above, and the MOI was 100:1. Extracellular bacteria were killed by adding lysozyme (10 μ g/mL). MG-63 or MC3T3-E1 cells in dishes were trypsinized, centrifuged, and suspended in 100 μ g/mL BODIPY®FL vancomycin (Thermo Fisher Scientific, USA). The concentration of the cell suspension was adjusted to 10⁶ cells/mL. Cells (1 \times 10⁶ cells/mL in 0.2 mL) were transferred to 1.5 mL polypropylene tubes and exposed to 400 shock wave impulses at 0.21 mJ/mm², with impulse rates of 3 Hz. Thereafter, half of the cell solution was transferred to a 12-well plate and incubated for 1 h, followed by 3 washings with PBS. After incubation, images were obtained under a fluorescence microscope (Olympus, Japan). For quantitative determination, another half of the cells were washed three times with PBS to remove extracellular BODIPY®FL vancomycin. Samples were then resuspended in PBS and sonicated for 2 min. Then the sonicated samples were centrifuged, and the absorbance of the supernatants in a 96-well black bottom plate was measured using a multifunctional microplate reader (BMG LABTECH, Germany).

2.2.6. Effect of shock waves on antibiotics entry into osteoblast models

Infected osteoblast models were developed as described above, and the MOI was 100:1. Extracellular bacteria were killed by adding lysozyme (10 μ g/mL). MG-63 or MC3T3-E1 cells in dishes were trypsinized, centrifuged, and suspended in vancomycin, cefuroxime sodium, rifampin, or levofloxacin (1 mg/mL). The concentration of the cell suspension was adjusted to 10⁶ cells/mL. Cells (1 \times 10⁶ cells/mL in 0.5 mL) were transferred to 1.5 mL polypropylene tubes and exposed to 400

shock wave impulses at 0.21 mJ/mm², with impulse rates of 3 Hz. Cells were washed three times with PBS to remove extracellular antibiotics. Samples were then resuspended in PBS and sonicated for 2 min. Thereafter, the sonicated samples were centrifuged, and the antibiotic accumulation in the supernatants was determined by high performance liquid chromatography-mass spectrometry (HPLC-MS) as previously described [27].

2.2.7. Effect of shock wave-assisted antibiotics on the clearance of *S. aureus* in osteoblast models

Infected osteoblast models were developed as described above, and the MOI was 100:1. Extracellular bacteria were killed by adding lysozyme (10 µg/mL). MG-63 or MC3T3-E1 cells in dishes were trypsinized, centrifuged, and suspended in vancomycin and cefuroxime sodium (1 mg/mL), respectively. The concentration of the cell suspension was adjusted to 10⁶ cells/mL. The cells (1 × 10⁶ cells/mL in 0.5 mL) were transferred to 1.5 mL polypropylene tubes and exposed to 400 shock wave impulses at 0.21 mJ/mm², with impulse rates of 3 Hz. Thereafter, cells were transferred to a 6-well plate and incubated for 24 h. After incubation, the intracellular viability of *S. aureus* was determined by lysing infected cells in 0.1 % Triton-X in PBS and plating the lysates on BHIA, followed by a visual count of bacterial colonies.

2.3. Mechanisms of shock wave-assisted antibiotic treatment of intraosteoblastic *S. aureus*

2.3.1. Antibacterial effect of extracorporeal shock waves

The bacterial suspension with an A600 of 0.5 was prepared and diluted to 5 × 10⁶ cells/mL with PBS. Bacterial suspension (5 × 10⁶ cells/mL in 0.5 mL) was transferred to 1.5 mL polypropylene tubes and exposed to 0, 50, 100, 150, 200, 250, 300, 350, 400, 450, 500, 550, and 600 shock wave impulses at 0.21 mJ/mm², with impulse rates of 3 Hz. The intracellular viability of *S. aureus* was determined by plating the lysates on BHIA followed by a visual count of bacterial colonies.

2.3.2. Measurement of extracellular ATP levels

Cells at 70–80 % confluency were resuspended at 1 × 10⁶ cells/mL. 0.5 mL of cell suspension was then transferred to 1.5 mL polypropylene tubes and exposed to 0, 100, 200, 300, 400, and 500 shock wave impulses at 0.21 mJ/mm², with impulse rates of 3 Hz. Afterward, cells were centrifuged at 1000×g for 5 min at 4 °C, and 100 µL of supernatant was transferred to a 96-well plate. 100 µL CellTiter-Lumi™ Plus Luminescent Cell Viability Assay Kit (Beyotime, China) were then added to each well and incubated for 10 min in the dark. The luminescent signal was measured with a multifunctional microplate reader (BMG LAB-TECH, Germany).

2.3.3. Evaluation of the toxic effects of ATP on osteoblasts

Infected osteoblast models were developed as described above, and the MOI was 100:1. Extracellular bacteria were killed by adding lysostaphin (10 µg/mL). MG-63 or MC3T3-E1 cells in dishes were trypsinized, centrifuged, and suspended in cell culture medium containing streptomycin/penicillin. The cell suspension was transferred to 48-well plates. 100 µL of different concentrations of ATP were then added to each well and incubated for 24 h. After incubation, the viability of cells was quantified with a CCK-8 assay kit (Beyotime, China).

2.3.4. Detection of P2X7 in osteoblasts by immunofluorescence

Immunofluorescence staining was performed to visualize the expression of P2X7 in osteoblasts. MG-63 and MC3T3-E1 cells were seeded in 6 cm-diameter dishes (1 × 10⁵ cells/dish) and incubated for 12 h. After washing with PBS, the cells were fixed with 3.7 % paraformaldehyde for 15 min. The resulting cells were incubated overnight with P2X7 receptor antibody (Alomone labs, Israel) at 4 °C, followed by PBS washing three times and Alexa Fluor 555-labeled Donkey Anti-Rabbit IgG (H + L) (Beyotime, China) incubation for 1 h at 37 °C in

the dark. The cells were washed gently and stained with DAPI (Beyotime, China). Finally, images were obtained under a fluorescence microscope (Olympus, Japan).

2.3.5. Effect of P2X7 receptor antagonists on the intracellular antibacterial effect of shock wave-assisted antibiotics

Infected osteoblast models were developed as described above, and the MOI was 100:1. Extracellular bacteria were killed by adding lysostaphin (10 µg/mL). MG-63 or MC3T3-E1 cells in dishes were trypsinized, centrifuged, and suspended in vancomycin and cefuroxime sodium (1 mg/mL), respectively. The concentration of the cell suspension was adjusted to 10⁶ cells/mL. 0.5 mL of cell suspension was added to a 1.5 mL Eppendorf tube and exposed to 400 shock wave pulses at impulse rates of 3 Hz in the presence or absence of the P2X7 receptor inhibitor KN-62 or A740003. Thereafter, cells were transferred to a 6-well plate and incubated for 24 h. After incubation, the intracellular viability of *S. aureus* was determined by lysing infected cells in 0.1 % Triton-X in PBS and plating the lysates on BHIA, followed by a visual count of bacterial colonies.

2.4. Rat osteomyelitis model

The induction of tibial osteomyelitis in rats is described in [Supplementary Methods 1.4](#).

2.5. Rat osteomyelitis treatment

2.5.1. Induction and treatment of tibial osteomyelitis

Male Wistar rats (12 weeks old) were randomly divided into six groups (n = 8): normal group (healthy rats without any treatment), bone defect group (bone defect inoculation with saline, no treatment after 1 month), control group (bone defect site inoculated with *S. aureus*, no treatment after 1 month), SW group (bone defect site inoculated with *S. aureus*, shock wave treatment after 1 month), Van group (bone defect site inoculated with *S. aureus*, vancomycin treatment after 1 month), Van + SW group (bone defect site inoculated with *S. aureus*, vancomycin combined with shockwave treatment after 1 month).

The rats were anesthetized with ketamine (10 mg/kg). After anesthesia, the hair was removed from the left hind legs, and the skin was disinfected. In the middle and upper thirds of the tibia, a cortical bone defect of 8 mm × 4 mm was made with a dental drill on a flat area, and 100 µL of *S. aureus* (ATCC25923) suspension (1 × 10¹¹ CFU/mL) was then inoculated into the medullary cavity of the defect to construct the osteomyelitis model. The bone defect group was inoculated with 100 µL of physiological saline.

At four weeks post-infection, the normal group, bone defect group, and control group were given no treatment; the SW group was given shockwave treatment; the Van group was given vancomycin treatment; and the Van + SW group was given shock wave-assisted vancomycin treatment. For vancomycin treatment, the rats were intraperitoneally injected with vancomycin solution (50 mg/kg) twice a day. For shock wave treatment, the rats were wrapped in a sterile medical dressing around the infected area, followed by filling the shock wave water bladder with water and then applying a medical coupling agent. Then the infected area was given an energy flow density of 0.21 mJ/mm², a frequency of 3 Hz, and 1500 shock wave treatments. The treatment was given once every 5 days, for a total of 6 times. The modeling and treatment procedures are shown in [Fig. S2](#).

2.5.2. General observation

At 0 weeks, 1 week, 3 weeks, and 5 weeks of treatment for osteomyelitis, the weights, body temperature, white blood cell count, and infected legs of the rats were recorded and photographed. The photographic results were scored according to the scoring system described by Petty et al. [28], with higher scores indicating more severe infection. After 5 weeks of treatment, the tibia was exposed after the execution of

the rats for observation and photography, and then scored according to the scoring system described by Rissing et al. [29].

2.5.3. Radiology evaluation

To observe bone defect healing and the inflammatory response at the site of bone infection, we acquired radiographic images (X-ray and MRI images) of the left tibias of rats at 0 weeks, 3 weeks and 5 weeks after the treatment for osteomyelitis. The collected anteroposterior X-ray images were assessed according to the scoring system described by Smeltzer et al. [30]. A higher score represented an increased severity of osteomyelitis. MRI analysis was performed with a 1.5 T unit (uMR580, Shanghai United Imaging Healthcare Co., Ltd.). Images were obtained on the sagittal, coronal, and axial planes. Intramedullary signal change, soft-tissue signal change, the presence of subperiosteal and/or extraperiosteal fluid, and soft-tissue abscess formation were examined. The infected tibias were detected via a micro-CT system (NMC-200, PINGSENG Healthcare Inc., China) at 5 weeks after osteomyelitis treatment. In addition, the three-dimensional digitized images were obtained through scan reconstruction. The BV/TV values were obtained via Avatar software (version 1.7.1, PINGSENG Healthcare Inc., China).

2.5.4. Microbiological and alkaline phosphatase evaluation

To determine the amount of bacteria in infected tibias, three rats in each group at 3 and 5 weeks after treatment were tested. The tibias were homogenized in saline with a TissueLyser (Shanghai Jinxin, China) after grinding and weighing 1 g. Viable bacteria in saline solution were serially diluted 10-fold and cultured in BHIA for 24 h at 37 °C, after which the bacteria were counted and photographed, and the number of bacteria per gram of tibia was calculated. In addition, Gram stain and plasma coagulase tests were performed on the cultured pathogenic bacteria. The above tissue grinds were centrifuged at 2000 rpm for 20 min, and the supernatant was collected, the level of alkaline phosphatase was quantified with a rat ALP ELISA kit (Sbjbio, China).

2.5.5. Histological analysis and immunohistochemical staining

Rats were euthanized at 5 weeks after treatment, and the tibia specimens were collected. Specimens were fixed with a 4 % paraformaldehyde solution for 24 h. After decalcification with 10 % EDTA solution for 1 month, specimens were embedded with paraffin wax, sectioned longitudinally, and deparaffinized for staining. The samples were sectioned to a thickness of 4 µm, and the bone defect region and three typical sections of the specimens were analyzed.

For H&E and Masson staining, the images were obtained by microscopy (NIKON ECLIPSE CI, USA). The stained sections were randomized and subsequently assessed for intraosseous acute inflammation (IAI), intraosseous chronic inflammation (ICI), periosteal inflammation (PI), and bone necrosis (BN) by a pathologist in a blind manner according to the scoring system described by Smeltzer et al. [30]. For immunohistochemical staining, the sections were stained with an anti-P2X7 receptor antibody. Then, an HRP-labeled anti-rabbit IgG was used as the secondary antibody for chromagen development. Color reactions were developed using the DAB substrate, and then the sections were counterstained with hematoxylin. The images were captured by a digital pathology system (3DHISTECH, Hungary).

2.5.6. In vivo safety

To observe the effects of shock wave-assisted antibiotic treatment on the liver and kidney functions of rats, the serum levels of aspartate aminotransferase (AST), alanine aminotransferase (ALT), urea (Ur) and creatinine (Cr) were measured 0 week, 1 week, 3 weeks and 5 weeks after treatment, respectively. At 5 weeks after treatment, major organs (heart, liver, spleen, lung, and kidney) were collected and fixed in 4 % paraformaldehyde for H&E analysis. Paraffin-embedded tissues were cut into 4 µm sections, and the images were captured by a digital pathology system (3DHISTECH, Hungary). Blood was collected from rats 30 min before and after shock wave treatment, and the blood was transferred to

a tube containing 15 mL of sterile TSB and incubated in a shaker at 37 °C for 24 h 100 µL of culture solution was inoculated on agar plates and incubated overnight at 37 °C for colony counting. Gram staining and plasma coagulase assays were performed on the cultured pathogenic bacteria.

2.6. Statistical analyses

The data were represented as the mean values ± standard deviations. Statistical analysis was performed with the Prism 9 software (GraphPad Software). The normal distribution was tested by Shapiro–Wilk test. If normality criteria were met, one-way ANOVA with posthoc multiple comparison test was run; if normality criteria were not met, the Kruskal–Wallis nonparametric test was run. (*p < 0.05, **p < 0.01, ***p < 0.001, ****p < 0.0001). The graphics in this manuscript were created using BioRender (<https://biorender.com/>) and Adobe Illustrator (version 2022).

3. Results

3.1. Validation of the effectiveness of shock wave-assisted antibiotics in the treatment of intraosteoblastic *S. aureus*

3.1.1. Establishment of intracellular *S. aureus* infection in (human and mouse) osteoblast models

The results of the intracellular *S. aureus* infection model are presented in [Supplementary Results 2.1](#). An MOI of 100 was the optimal infection multiplicity for *S. aureus* infection of osteoblasts MG-63 and MC3T3-E1 and was used in the subsequent experiments.

3.1.2. Extracorporeal shock waves exposure

The damage effects of a specific number of shock waves on the osteoblast model are presented in [Supplementary Results 2.2](#). The shock wave parameters of 0.21 mJ/mm², 3 Hz, and 400 impulses were selected for the following experiments.

3.1.3. Effect of shock waves on osteoblasts in antibiotic solution

The effect of shock waves on osteoblasts in antibiotic solution is presented in [Supplementary Results 2.3](#). The osteoblasts in culture with vancomycin, cefuroxime sodium, rifampin, or levofloxacin (1mg/mL) had standard cell morphology and proliferation in the SW and Con groups after 24 h of shock wave treatment, and no significant extracellular bacterial growth was observed.

3.1.4. Effect of shock waves on cell membrane permeability in the intracellular *S. aureus* infection model

To determine the effects of shock wave treatment on cell membrane permeability, MG-63 and MC3T3-E1 cell models were treated with shock waves as described above in the presence of BODIPY®FL vancomycin, and cellular uptake of BODIPY®FL vancomycin was assessed by fluorescence microscopy. In MG-63 and MC3T3-E1 cells, the fluorescence intensity was significantly higher in the SW group compared with the Con group, revealing a significant increase in intracellular vancomycin levels ([Fig. 2A](#)). Quantitative analysis also revealed that the intracellular BODIPY®FL vancomycin levels in the SW group were significantly higher than those in the Con group (p < 0.001) ([Fig. 2A](#)). This result suggests that shock waves can alter the permeability of the cytosolic membrane of the osteoblasts and induce the entry of BODIPY-FL-labeled vancomycin into the cells.

3.1.5. Shock waves promote the entry of antibiotics into osteoblasts and enhance intracellular antibacterial activity

Based on the above findings, we explored whether shock waves can promote the entry of antibiotics into osteoblasts. We incubated MG-63 and MC3T3-E1 cell models with 1 mg/mL of different antibiotics, followed by 400 shock wave impulses at 0.21 mJ/mm². Then, we

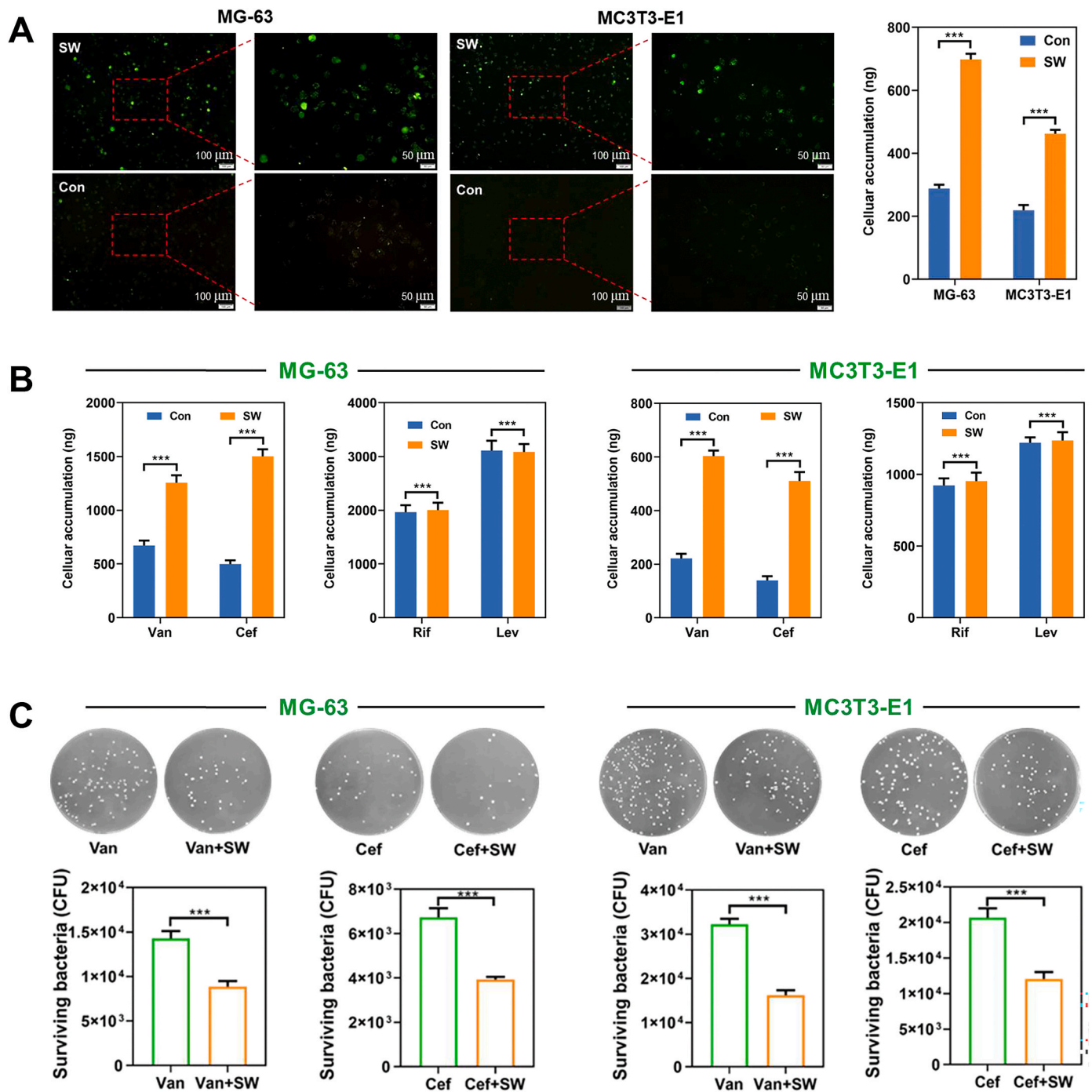


Fig. 2. Shock waves can induce the permeabilization of osteoblasts, and then promote vancomycin and cefuroxime sodium to enter the cells and exert antibacterial effects (A) BODIPY®FL vancomycin was used to evaluate the effect of shock wave treatment on cell membrane permeability in the osteoblast model cells (B) Effect of shock wave treatment on antibiotics entry into osteoblast model cells (C) Effect of shock wave-assisted antibiotics on the clearance of *S. aureus* in osteoblast model cells. Data are presented as mean ± SD. **p* < 0.05, ***p* < 0.01, ****p* < 0.001; ns, not statistically significant.

determined the intracellular antibiotic concentrations by using HPLC. Shock wave treatment was able to significantly induce the hydrophilic antibiotics vancomycin and cefuroxime sodium into osteoblasts MG-63 and MC3T3-E1 (*p* < 0.001), while it had insignificant effects on the lipophilic antibiotics rifampicin and levofloxacin (*p* > 0.05) (Fig. 2B). After treatment, the intracellular viability of *S. aureus* was determined by plating the lysates on BHIA followed by a visual count of bacterial colonies. Compared with that in the control group, the intracellular *S. aureus* count in the vancomycin shock wave (SW) group decreased by approximately 5400 cfu/well in MG-63 cells and 16,067 cfu/well in

MC3T3-E1 cells at 24 h after shock wave treatment. In the cefuroxime sodium shock wave (SW) group, the intracellular *S. aureus* count decreased by approximately 2800 cfu/well in MG-63 cells and 8600 cfu/well in MC3T3-E1 cells at 24 h after shock wave treatment when compared with that in the control group (Fig. 2C). These results indicated that shock wave treatment could promote the delivery of vancomycin and cefuroxime sodium into osteoblasts and improve the intracellular antibacterial activity of the two antibiotics.

3.2. Mechanisms of shock wave-assisted antibiotic treatment of intraosteoblastic *S. aureus*

First, we applied the plate colony counting method to evaluate the effect of different shock wave impulses on *S. aureus* to exclude the direct killing effect of shock wave treatment on bacteria. Shock waves with an energy density of 0.21 mJ/mm² and a frequency of 3 Hz did not have a significant damaging effect on *S. aureus* within a number of 2500 impulses (Fig. 3A). This result suggested that the reduction of intracellular *S. aureus* by antibiotics at 400 shock wave impulses was not caused by the direct killing of *S. aureus* by shock wave treatment.

We studied whether ATP release played a role in the mechanisms behind the improvement of antibiotic delivery by shock wave treatment. Using P2X7-specific antibodies, we first checked to see if P2X7 receptors were present on the cell surfaces of MG-63 and MC3T3-E1. We discovered that MG-63 and MC3T3-E1 had highly expressed P2X7 receptors using immunofluorescence labeling (Fig. 3B). To evaluate whether shock waves stimulate ATP release, shock wave treatment was applied to MG-63 and MC3T3-E1 cells, and extracellular ATP concentrations were measured using an ATP assay. It was found that the extracellular ATP concentrations of MG-63 and MC3T3-E1 cells were significantly increased after the shock wave treatment, and the ATP concentration increased as the shock wave impulses increased (Fig. 3C). Next, we treated MG-63 and MC3T3-E1 cells with ATP and assessed cell viability using the CCK-8 assay. As shown in Fig. 3D, ATP at concentrations ≤10 μM did not noticeably affect cell viability. However, ATP concentrations ≥100 μM significantly reduced cell viability (p < 0.05) (Fig. 3D). These findings imply that ATP release does not contribute to cell death given that shock wave-induced extracellular ATP concentrations were less than 10 μM.

According to the studies above, shock wave treatment opens channels in cell membranes to make it easier for antibiotics to enter cells. To test this hypothesis, we administered vancomycin or cefuroxime sodium to MG-63 and MC3T3-E1 cells in the presence or absence of the P2X7 receptor inhibitors KN-62 or A740003, and then measured intracellular antibacterial activity after shock wave treatment. We found that intracellular antibacterial activity was significantly weakened by KN-62 or A740003 treatment (p < 0.05) (Fig. 4A and B), which indicates that P2X7 receptors are required for the shock wave-mediated enhancement of intracellular antibacterial activity. These findings imply that shock wave treatment increased intracellular antibacterial activity via increasing antibiotic consumption by modifying cell membrane permeability via P2X7 receptor-ATP signaling.

3.3. Rat osteomyelitis model

The results of the rat osteomyelitis model are presented in [Supplementary Results 2.4](#). In the group inoculated with saline, no rats were infected after 4 weeks, indicating that the aseptic surgical operation was successful. When inoculated with 0.1 mL 1 × 10⁷ CFU/mL bacterial suspension, the infection rate was 40 % after 4 weeks, no rats died, and the infected rats had mild signs of infection and mild imaging and pathological chronic osteomyelitis changes at the surgical site. When inoculated with 0.1 mL of 1 × 10⁹ CFU/mL bacterial suspension, the infection rate of rats was 100 % after 4 weeks, with no rat deaths, mild signs of infection, and mild to moderate imaging and pathological chronic osteomyelitis changes at the surgical site. When inoculated with 0.1 mL of 1 × 10¹¹ CFU/mL bacterial suspension, the infection rate in rats was 100 % after 4 weeks, with no rat deaths, severe signs of infection, and severe imaging and pathological chronic osteomyelitis changes

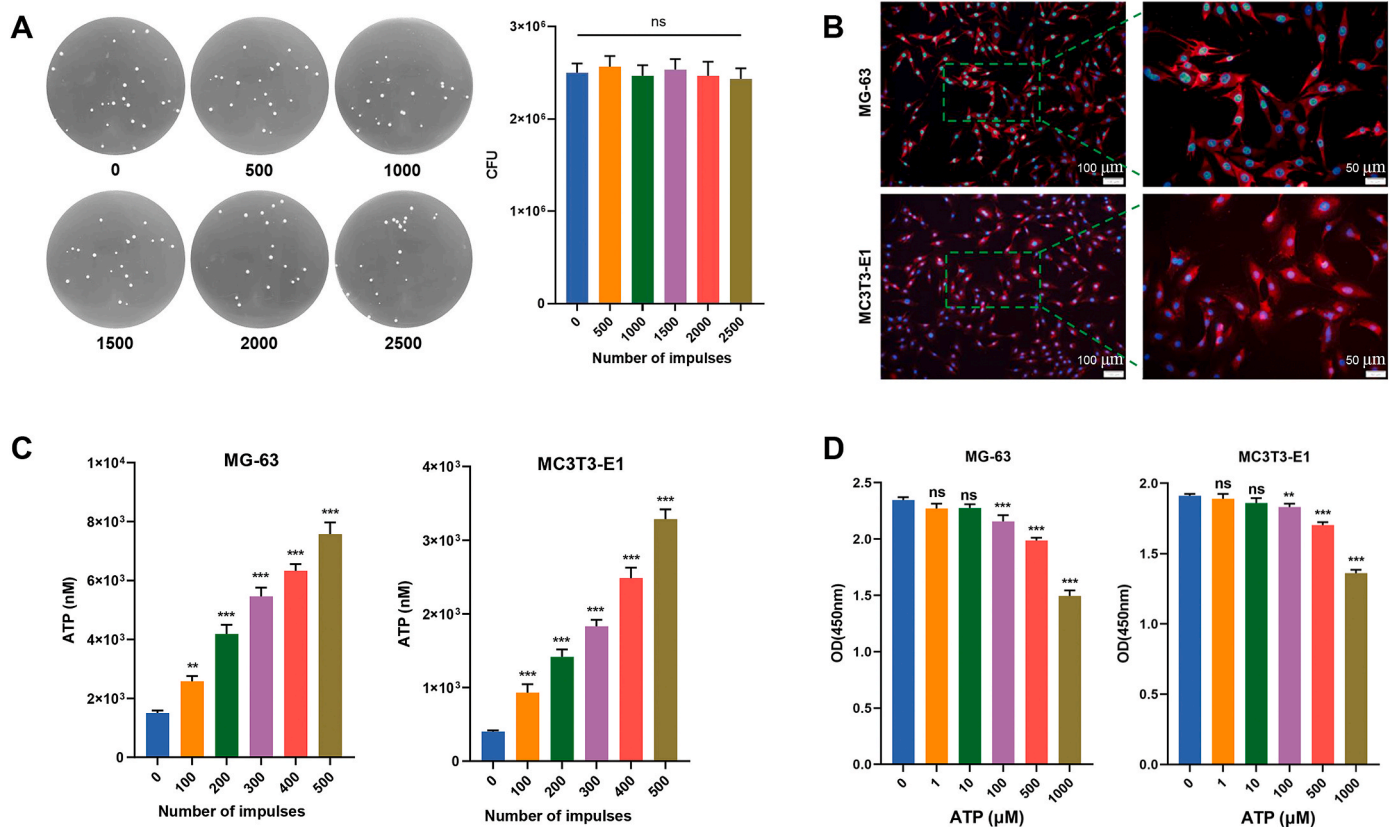


Fig. 3. (A) There was no antibacterial effect of extracorporeal shock waves (B) P2X7 receptors were highly expressed on the cell surface of MG-63 and MC3T3-E1 cells (C) Shock wave treatment increased the extracellular concentration of ATP in MG-63 and MC3T3-E1 cells (D) MG-63 and MC3T3-E1 cells were treated with the indicated concentrations of ATP and cell viability was assessed by the CCK-8 assay. Data are presented as mean ± SD. *p < 0.05, **p < 0.01, ***p < 0.001; ns, not statistically significant.

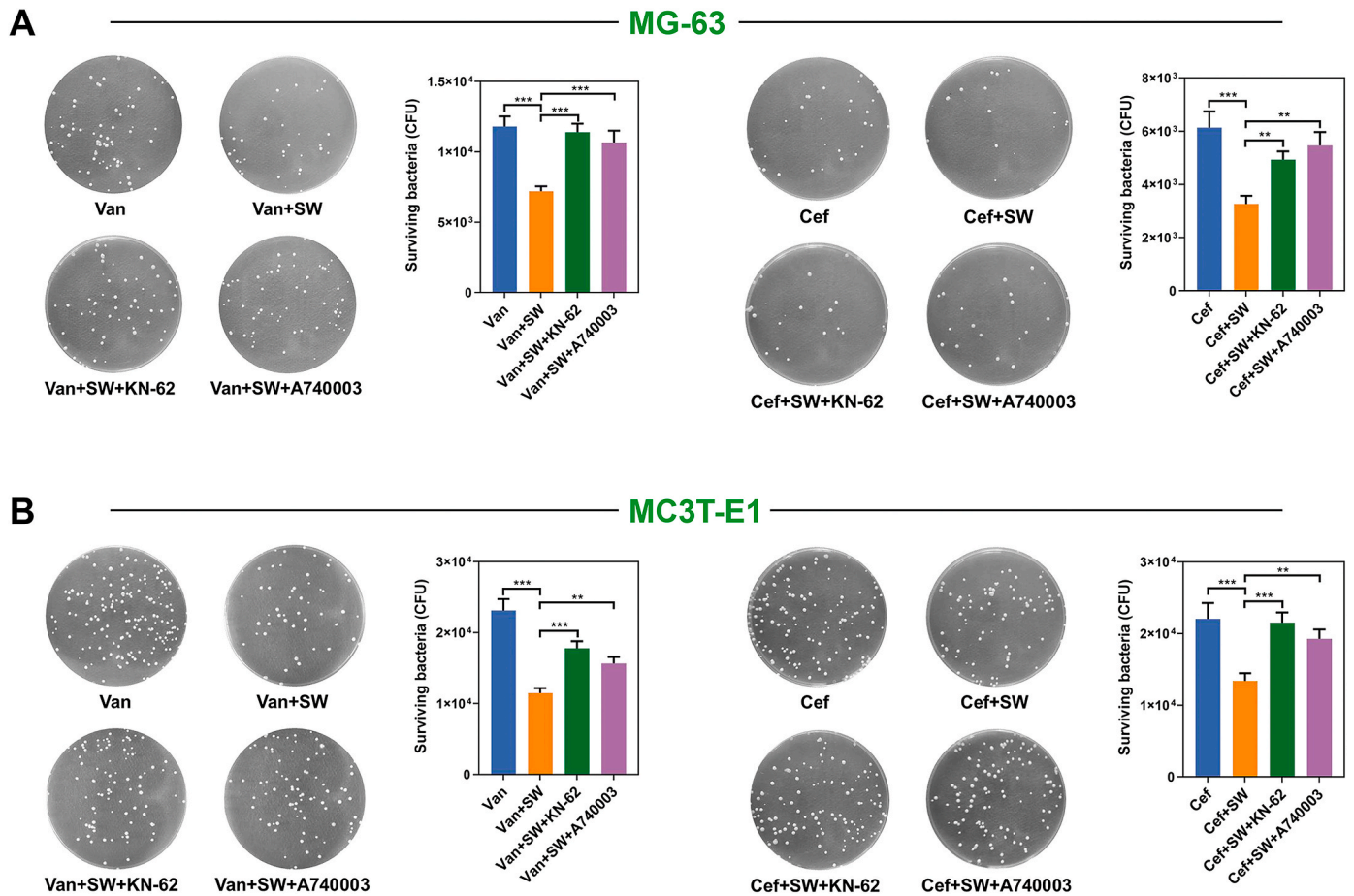


Fig. 4. Effect of P2X7 receptor antagonists on the intracellular antibacterial effect of shock wave-assisted antibiotics. Data are presented as mean ± SD. *p < 0.05, **p < 0.01, ***p < 0.001; ns, not statistically significant.

at the surgical site. When inoculated with 0.1 mL of 2×10^{11} CFU/mL bacterial suspension, the infection rate of rats was 100 % after 4 weeks, with severe symptoms of infection, severe weight loss of rats, 2 rats deaths, and severe imaging and pathological chronic osteomyelitis changes at the surgical site. The concentration of *S. aureus* was the key to the success of chronic osteomyelitis modeling; too much bacteria led to the death of rats and too few bacteria did not cause osteomyelitis in rats. By comparing the five groups of rats, we found that 0.1 mL of 1×10^{11} CFU/mL of ATCC25923 *S. aureus* is suitable for modeling chronic osteomyelitis in rats, so we will choose 0.1 mL of 1×10^{11} CFU/mL of bacterial suspension at the cortical bone defect as the bacterial dose for modeling chronic osteomyelitis in rats in subsequent experiments.

3.4. Rat osteomyelitis treatment

After the successful establishment of chronic osteomyelitis in rats, the therapeutic effect of shock wave-assisted vancomycin on rat osteomyelitis was investigated (Fig. 5A).

3.4.1. General observations

From the images of the surgical sites (Fig. 5B), at 0 weeks, the infected legs of rats in the control, SW, Van, and Van + SW groups exhibited severe abscesses from the sinus tract, while the legs in the normal, bone defect group had no abnormal change. At three and five weeks, the infected legs of rats in the control and SW groups still exhibited severe abscesses from the sinus tract, while the skin abscesses of legs in the Van and Van + SW groups were almost completely ameliorated. In addition, when we surgically incised the infected skins, it can be observed that the bone defects of infected rats exhibited

festering in the Van group, while the Van group were normal without festering, suggesting a considerable suppression of infection.

In addition, the body weight change of rats was recorded during the 5 weeks. Van and Van + SW groups rats exhibited a healthy increasing trend in body weight; however, the control and SW groups rats gained weight at a slower rate due to the infection (Fig. 5C). Moreover, body temperature and white blood cell (WBC) counts of the Van + SW group returned to normal faster compared those of the Van groups (Fig. 5D and E), indicating that the systemic inflammation response was also relieved after shock wave-assisted vancomycin treatment.

3.4.2. Radiographic analyses

Digital X-ray and MRI of the left tibias of the rats are shown in Fig. 6. At 0 week after treatment, the radiographic images confirmed the presence of osteomyelitis, along with osseous destruction and stimulation of bone formation by the periosteal reaction (Fig. 6A, X-ray, control, SW, Van, and Van + SW groups); the MRI revealed changes in the intramedullary signal belonging to osteomyelitis areas and an abscess of soft tissue (Fig. 6B, MRI, control, SW, Van, and Van + SW groups). Three to five weeks after treatment, infection developed as manifested by the progressive inflammation and bone destruction, and periosteal reactions and large sequestrum formations were also observed (Fig. 6A, X-ray, in the control, SW, and Van groups). The MRI revealed cortical bone thickening resulting from abscess formation, subperiosteal and extraperiosteal fluid, and swelling of soft tissue (Fig. 6B, MRI, in the control, SW, and Van groups). In the Van + SW group, a slight periosteal reaction occurred without bone abscess, and the bone defect was obviously repaired (Fig. 6A and B, X-ray and MRI). The mean radiographic scores of Van + SW group animals were also significantly lower than those of

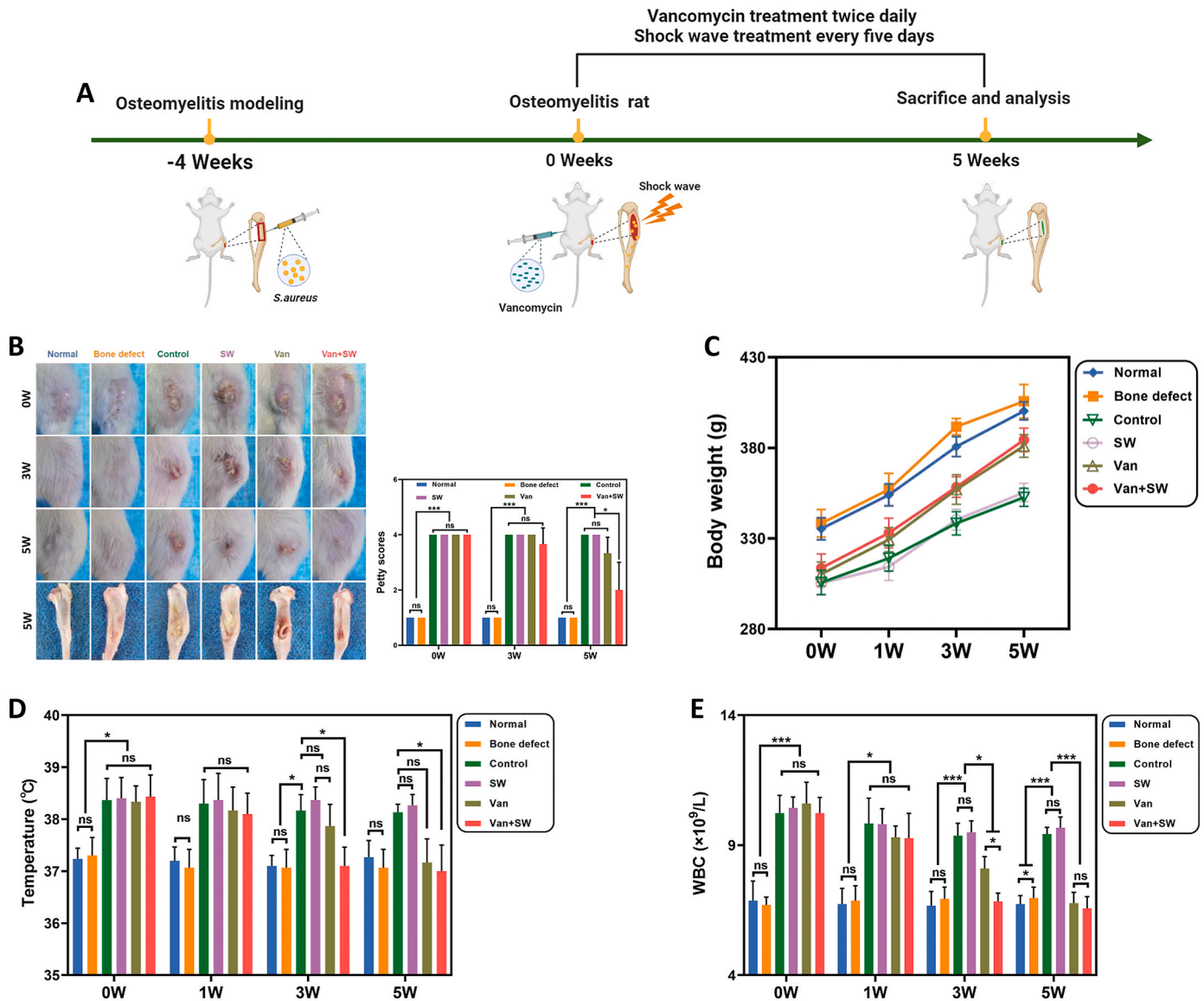


Fig. 5. (A) Schematic illustration of the establishment and treatment of osteomyelitis model rats (B) Surgical site images and Petty scores of rats with osteomyelitis before and after treatment (C) Changes in the body weight of rats with osteomyelitis in each group before and after treatment (D) Changes in the body temperature of rats with osteomyelitis before and after treatment (E) White blood cell (WBC) counts of rats with osteomyelitis before and after treatment in each group.

the control, SW, and Van groups.

To observe the change in bone mass after treatment, micro-CT detection was conducted to monitor the infected tibia. As shown in Fig. 6C, large bone defects were observed in the control and SW groups resulting from osteomyelitis, whereas the Van and Van + SW groups showed a much smaller bone defect area, and the reduction of bone defects in the Van + SW group was more significant than that in the Van group, which was further confirmed by the bone volume/total volume (BV/TV) of the tibia defect (Fig. 6C) and Masson staining (Fig. 7B).

3.4.3. Microbiological and alkaline phosphatase evaluation

After 3 and 5 weeks of treatment, 3 tibia were taken from each group. Homogenized tibias from the infectious legs were added to BHIA plates to evaluate the therapeutic efficacy of the treatments by performing bacterial counts. The results showed that there was no bacterial infection in the tibia of rats in the normal and bone defect group (Fig. 7A), indicating that the aseptic operation was successful and did not cause bacterial infection in rats. The bacterial load in the tibia of rats in the SW group was not significantly different from that in the tibia of rats in the control group ($p > 0.05$). The bacterial load in the tibia of rats in the Van

and Van + SW groups was significantly lower than that in the tibia of rats in the control group ($p < 0.05$), indicating that vancomycin treatment could significantly reduce the number of bacteria at the site of infection, and the effect of shock wave treatment alone was not obvious. In addition, compared with that in the Van group, the bacterial load in the Van + SW group was more significantly decreased ($p < 0.05$), suggesting that shock wave treatment can increase the antibacterial activity of vancomycin.

To further examine the osteogenesis in the osteomyelitis bone defect area of rats, we examined the expression of the osteogenesis-related protein ALP in the bone defect area (Fig. 6D). The results showed that after 3 and 5 weeks of treatment, the expression levels of ALP in the SW group were not significantly different from those in the control group ($p > 0.05$), indicating that shock wave treatment alone did not have a significant effect on osteogenesis in the bone defect area of osteomyelitis. The expression levels of ALP in the bone defect, Van, and Van + SW groups were significantly higher than those in the control group ($p < 0.01$), indicating that there was significant osteogenic activity in the bone defect, Van, and Van + SW groups, which may be related to the absence of bacterial infection in the bone defect group, and the decrease

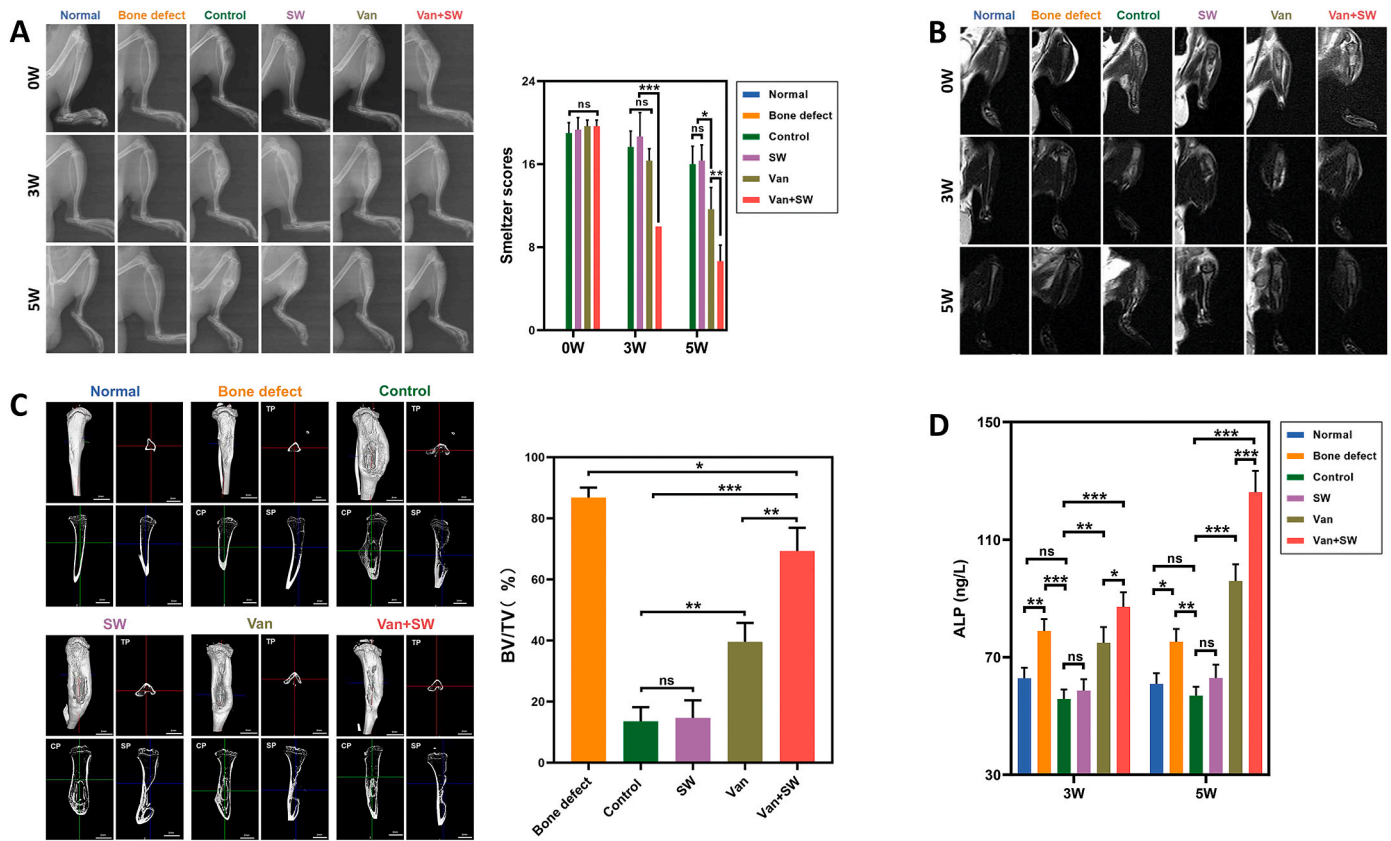


Fig. 6. (A) Digital X-ray and radiographic scores of the left tibia of rats in the five groups (B) MRI of the left tibia of rats in the five groups (C) Micro-CT images and BV/TV values of the left tibia of rats in the five groups (D) The level of alkaline phosphatase in the bone defect area of osteomyelitis model rats. Data are presented as the mean ± SD. *p < 0.05, **p < 0.01, ***p < 0.001; ns, not statistically significant.

of bacterial load and the improvement of the inflammatory environment in the Van and Van + SW groups. The ALP expression level was higher in the Van + SW group compared with the Van group (p < 0.05), suggesting a stronger osteogenic response in the Van + SW group compared with the Van group. Based on the above results, we know that the application of vancomycin can promote the osteogenic response in the bone defect area of osteomyelitis model rats, and shock wave-assisted vancomycin treatment can significantly enhance the osteogenic response. However, shock wave treatment alone has no significant osteogenic effect in the bone defect area of osteomyelitis model rats.

3.4.4. Histological evaluation

The HE- and Masson-stained rat tibia tissue sections are shown in Fig. 7B. Five weeks after treatment, osteomyelitis with massive sequestrum (red arrow), abscess (yellow arrow), and large bone defects were observed, and large inflammatory cell infiltration ascribed to bacterial infection appeared in the medullary cavity (Fig. 7B, HE and Masson, control, and SW groups). In addition, the inflammatory cell infiltration and bone defects were reduced, but sequestrum (red arrow) and abscess (yellow arrow) were still observed (Fig. 7B, HE and Masson, Van group). In the Van + SW group, the bone infection by *S. aureus* was suppressed, and the sequestrum and abscesses were absent. Moreover, the infected tibias showed a much lower bone defect area with only a slight observed inflammatory reaction (Fig. 7B, HE, Van + SW group). The histological score of the Van + SW group was significantly lower than that of the control, SW, and Van groups. To further investigate the expression of P2X7 receptors in infected tissues, immunohistochemical staining was also performed after 5 weeks of treatment. A large number of P2X7 receptors were expressed in the bone tissues of rats in all groups, both in new and healthy bone tissues, and even in the inflamed tissues of the bone defect areas (Fig. 7B, IHC).

4. Discussion

S. aureus invades osteoblasts and resides within the cells, overcoming host immune clearance and antibiotic treatment and thus prolonging their inside the cells. The intracellular *S. aureus* causes apoptosis and necrosis in osteoblasts, and the released *S. aureus* infects other osteoblasts and eventually causes recurrent infections in bone tissue. Therefore, how to effectively deliver antibiotics to kill bacteria in osteoblasts is a challenge in the treatment of chronic osteomyelitis. Although nanoparticles loaded with antibiotics have been experimentally shown to have suitable efficacy in the treatment of intracellular bacteria, they have not been used in the clinical treatment of patients with chronic osteomyelitis due to safety and cost reasons.

A large number of studies have reported that shock waves that do not affect cell viability can temporarily increase the permeability of the cell membrane and cause extracellular macromolecular substances to enter the cell [31,32]. Kodama et al. [31] found that calcein and fluorescein isothiocyanate-dextran (FITC-D) could be effectively transferred into HL-60 cells (human promyelocytic leukemia cells) by shock wave treatment, while the viability of cells remained >95 %. The molecular weight of calcein and FITC-D were 622 Da and 71,600 Da, respectively. The molecular weights of vancomycin, cefuroxime sodium, levofloxacin and rifampicin were 1449.25 Da, 446.37 Da, 361 Da and 822.94 Da, respectively, which were close to calcein and much smaller than FITC-D. Therefore, we hypothesized that shock waves could improve the entry of the four antibiotics into osteoblasts without affecting cell viability. In this study, we demonstrated that subjecting cells to low shock wave treatment does not significantly decrease MG-63 and MC3T3-E1 cell viability. We found that the viability of MG-63 and MC3T3-E1 cells remained >95 % following ≤400 shock wave impulses at 0.21 mJ/mm², which were used for further experiments. Shock wave treatment

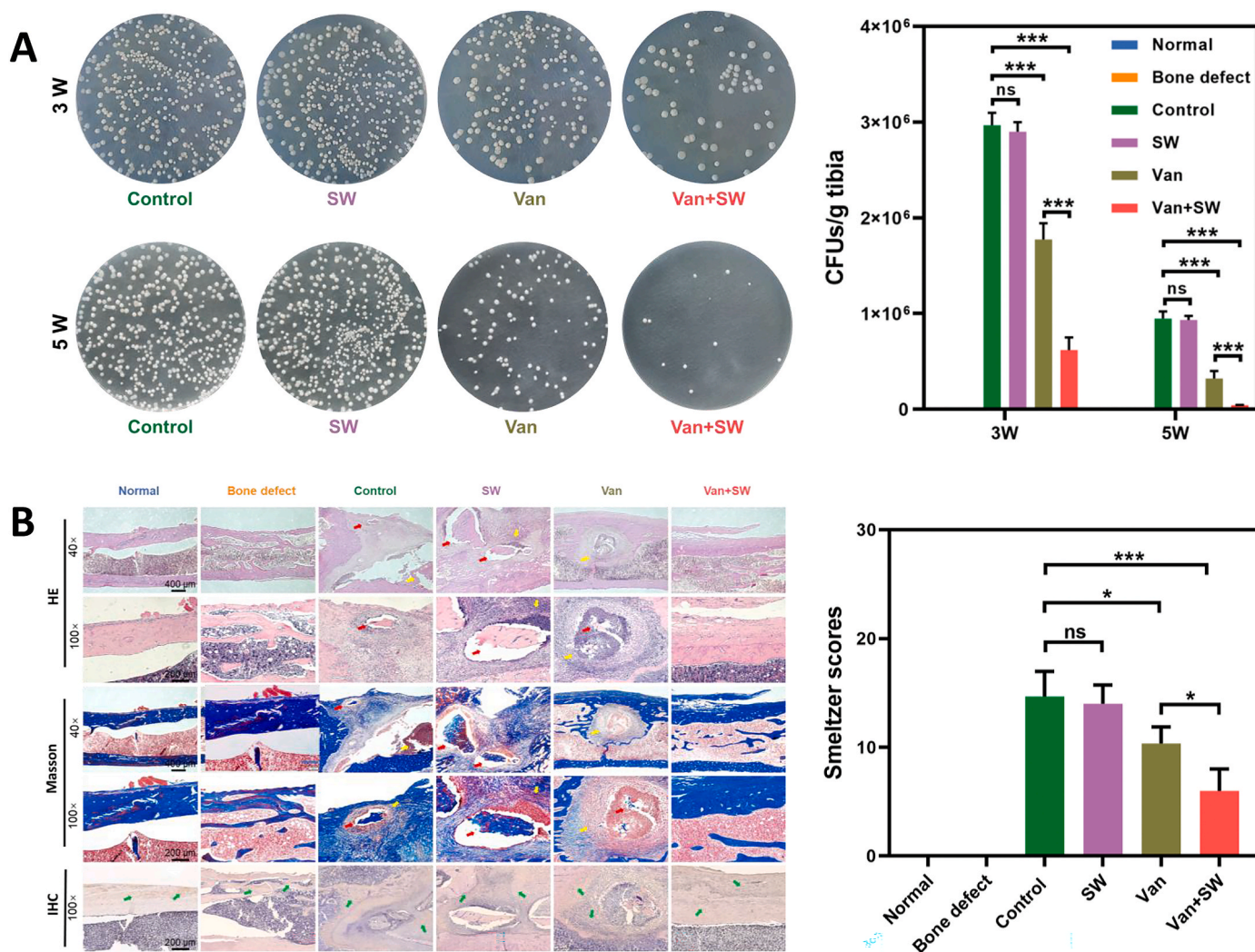


Fig. 7. (A) The bacterial load in the tibia of osteomyelitis model rats after five weeks of treatment (B) The hematoxylin-eosin (HE) staining and Masson staining of longitudinal sections, and the histological scores of the left tibia of rats in the five groups after five weeks of treatment.

significantly promoted the delivery of BODIPY-FL-labeled vancomycin (molecular weight: 1723.35 Da), suggesting that shock waves can increase transient cell membrane permeability. More importantly, we also found that shock waves were able to significantly induce the hydrophilic antibiotics vancomycin and cefuroxime sodium to enter osteoblasts MG-63 and MC3T3-E1, enhancing the intracellular antibacterial effects of these two antibiotics. In contrast, the effect of shock waves on the lipophilic antibiotics rifampicin and levofloxacin was not significant. This observation may be because lipophilic antibiotics themselves can easily enter the cells, making the shock wave promotion of intracellular entry of levofloxacin and rifampicin insignificant.

Previous experiments have found that P2X7 receptors are expressed on the membrane of human osteoblasts and mouse osteoblasts [33–35]. When high extracellular ATP binds to P2X7 receptors, P2X7 receptors increase the permeability of the cell membrane to macromolecules by expanding their own pore size [36] or activating another nonselective macropore-forming protein [37], which is referred to as the macropore-forming mechanisms. P2X7 receptors belong to the P2X receptor family, a type of purinoceptor [38], and are widely distributed in neurons, glial cells, epithelial cells, endothelial cells, bone, muscle, and other tissue cells [39]. Purinoceptors are divided into two groups: the P1 receptors, which are divided into four main subtypes (A1R, A2aR, A2bR, and A3R) and are mainly activated by adenosine, and the P2 receptors, which consist of two main families, P2X and P2Y, and are responsive to

nucleotides [40]. P2X7 receptor channels are able to switch between two open states depending on the activation conditions. The small molecule opening of P2X7 receptor channels involves the basal activation of P2X7 receptors leading to the opening of membrane channels to small molecule cations (such as Ca²⁺, K⁺, and Na⁺) [39]. The macromolecular opening of P2X7 receptor channels involves the prolonged exposure of P2X7 receptors to high concentrations of ATP (≥100 μM) during mechanical stress and tissue trauma, which causes enlargement of the cell membrane pore and leads to the passage of macromolecular substances (molecular weight ≥900 Da) through the cell membrane [41]. We further found that P2X7 receptors were highly expressed on the surface of MG-63 and MC3T3-E1 cells, and found that shock wave treatment increased the extracellular concentration of ATP, which did not noticeably affect cell viability. Moreover, we treated MG-63 and MC3T3-E1 models with vancomycin or cefuroxime sodium in the presence or absence of the P2X7 receptor inhibitor KN-62 or A740003, and then assessed intracellular antibacterial activity following shock wave treatment. We found that intracellular antibacterial activity of shock wave assisted with antibiotic treatment was significantly weakened by KN-62 or A740003, which indicates that P2X7 receptors are required for the enhancement of intracellular antibacterial activity by shock waves. In summary, the proposed mechanism by which shock waves enhance the entry of vancomycin and cefuroxime sodium into osteoblasts is as follows: shock wave treatment induces ATP release from MG-63 and

MC3T3-E1 cells, extracellular ATP then binds the P2X7 receptor to increase the permeability of cell membrane, thus allowing vancomycin and cefuroxime sodium to enter the cell and exert antibacterial effects (Fig. 8).

Currently, clinicians often use high doses of antibiotics to treat patients with chronic osteomyelitis [42], among which vancomycin is a commonly used antibiotic for the treatment of chronic osteomyelitis caused by *S. aureus*. Therefore, in the vivo experiments, we chose to treat chronic osteomyelitis of the tibia in rats by direct intraperitoneal injection of vancomycin and or shock wave treatment. The most important treatment for chronic osteomyelitis is to kill bacteria in osteomyelitis bone and control bone destruction caused by bacterial infection. Bacterial counting after grinding bone at the osteomyelitis site is the most common detection method to determine bacterial load [43,44]. Vancomycin treatment alone was found to reduce the bacterial load at the site of osteomyelitis in rats, and shock wave-assisted vancomycin treatment resulted in a more significant reduction in the bacterial load at the site of osteomyelitis. Imaging is an important tool in the evaluation of chronic osteomyelitis, not only to observe the degree of infection at the infected site but also to determine bone healing. We found that rats treated with vancomycin showed reduced inflammatory response and reduced bone defects on X-ray, Micro-CT and MRI scans, and the reduction of inflammation and bone defects was more obvious in rats treated with shock wave-assisted vancomycin, while there was no significant improvement in inflammation and bone defects in rats in the control and shockwave groups without vancomycin treatment. ALP plays an important role in the osteogenesis process and can directly reflect the activity of osteoblasts. ALP activity measurements in the bone defect area can be used to determine the degree of osteogenesis in the bone defect area [45]. The results revealed that the highest level of ALP expression was found in rats treated with shock wave-assisted vancomycin. The results of the HE and Masson staining were consistent with the imaging results, and shock wave-assisted vancomycin treatment of chronic osteomyelitis in rats had significant anti-bacterial and osteogenic effects. In addition, IHC analysis showed that a large number of

P2X7 receptors were expressed in the bone tissue of rats. We speculated that the ATP/P2X7 pathway may be involved in the treatment of chronic osteomyelitis in rats with shock wave assisted antibiotics. The study revealed that shock wave-assisted vancomycin treatment can significantly promote bone healing in the bone defect area of osteomyelitis in rats. This effect may be related to a significant reduction of the bacterial load at the site of osteomyelitis and a significant improvement of the inflammatory microenvironment at the site of osteomyelitis, creating favorable conditions for osteogenic activity. Moreover, shock wave treatment may increase the osteogenic differentiation of bone marrow mesenchymal stem cells (BMSCs) at the site of osteomyelitis by activating P2X7 receptors in the inflammatory state. In the noninflammatory state, shock wave treatment has been shown to promote the osteogenic differentiation of BMSCs by activating P2X7 receptors [38]. In addition, it has been shown that inflammation significantly inhibits P2X7 receptor expression and the osteogenic differentiation ability of periodontal ligament stem cells, but P2X7 receptor activation can significantly enhance the osteogenic differentiation ability of periodontal ligament stem cells inhibited by inflammation [46].

Studies have shown that shock wave-assisted vancomycin can effectively treat chronic osteomyelitis in rats, but safety also needs to be considered. Daily intraperitoneal injections of a high concentration of vancomycin may produce toxic and side effects on the liver and kidney function and the body of rats. Moreover, shock wave treatment may cause the spread of bacteria from the site of tibial osteomyelitis to the whole body in rats, aggravating the infection. Based on these two considerations, blood samples were collected from each group 1 day before treatment and at 1, 3, and 5 weeks of treatment for liver and kidney function tests. The results showed that vancomycin treatment alone did not further damage the liver and kidney function of rats, and instead improve their liver and kidney function of rats. Shock wave-assisted vancomycin treatment could quickly improve the liver and kidney function of rats, but shock wave treatment alone had no significant improvement. In addition, the important internal organs of rats in each group were collected for histopathological examination after 5 weeks of

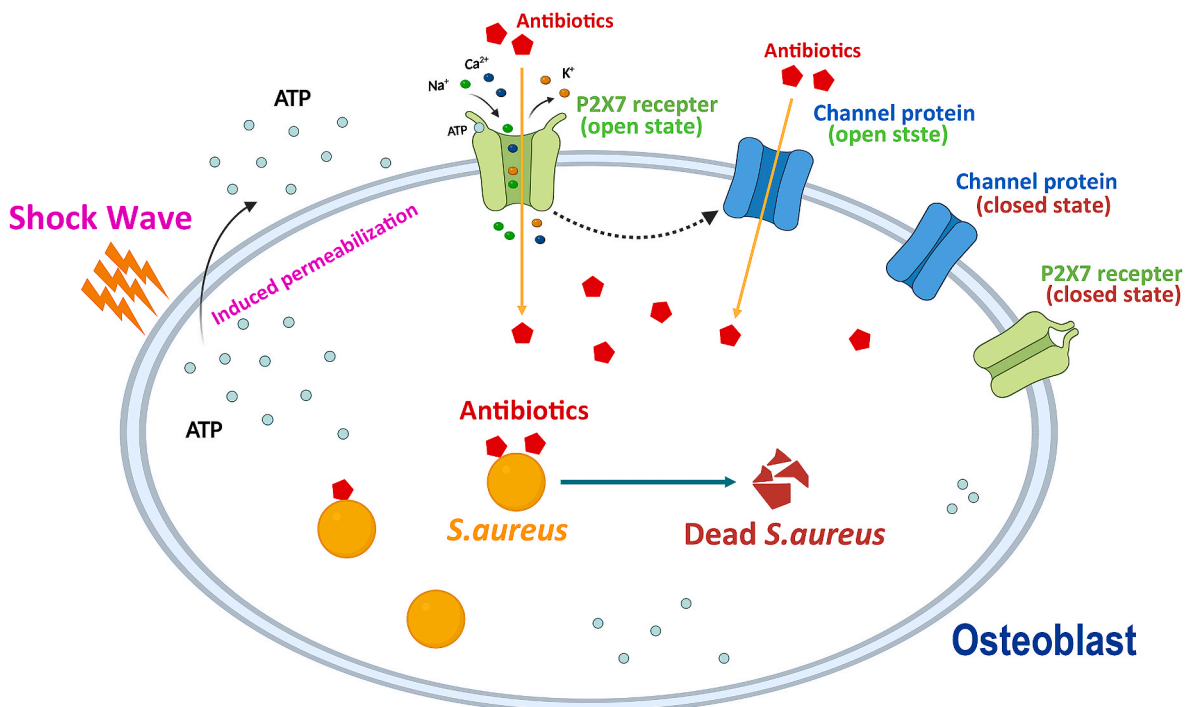


Fig. 8. The mechanism hypothesized for shock wave-assisted antibiotics against intraosteoblastic *S. aureus*. Shock wave treatment causes intracellular ATP to be released, followed by binds P2X7 receptors, which contribute to the opening of cell membrane channels, allowing antibiotics to enter the cells and kill intraosteoblastic *S. aureus*.

treatment. The results showed that the heart, liver, spleen, lung, and kidney of each group showed normal tissue morphology, which proved that the dose of vancomycin used in this experiment had no obvious toxic and side effects on the important internal organs of rats. No *S. aureus* was found in blood cultures before and after shock wave treatment, indicating that the treatment did not cause the bacteria to spread to the whole body and aggravate the infection in tibial osteomyelitis model rats.

Our study has several limitations. First, whether the effectiveness of shock-wave assisted antibiotics in the treatment of *S. aureus* infection in osteoblasts is present in vivo needs to be further verified using transgenic animals. Second, whether shock wave combined with antibiotics has a suitable therapeutic effect on patients with chronic osteomyelitis needs further study. Finally, whether shock waves activate the osteogenic differentiation potential of BMSCs suppressed by inflammation via the P2X7 receptor pathway needs to be further investigated.

5. Conclusion

We report a novel intracellular anti-infection method for the treatment of osteomyelitis caused by *S. aureus* infection. The effectiveness of shock wave-assisted vancomycin against intraosteoblastic *S. aureus* was demonstrated in vitro, and the mechanism was related to the ATP/P2X7 receptor pathway. Moreover, shock wave-assisted vancomycin successfully treated MRSA-infected osteomyelitis in vivo. We also preliminarily ascertained the safety of shock wave-assisted vancomycin treatment; in particular, this treatment induced no local or systemic side effects and no signs of bacteremia occurred. This work provides a feasible strategy for the treatment of osteomyelitis.

Data availability

Data will be made available on request.

Authorship

Conception and design of study: T.C. Yu, J.B. Li; Acquisition of data: J.B. Li, H.X. Li, S.Q. Bi, Y. Sun, Analysis and/or interpretation of data: J. B. Li, H.X. Li, F. Gu. Drafting the manuscript: J.B. Li. Revising the manuscript critically for important intellectual content: T.C. Yu, J.B. Li, H.X. Li; Approval of the version of the manuscript to be published : J.B. Li, H.X. Li, S.Q. Bi, Y. Sun, F. Gu, T.C. Yu.

Article Processing Charge

The corresponding author agrees to pay the Journal of Orthopaedic Translation Article Processing Charge upon acceptance of the work for publication in Journal of Orthopaedic Translation.

Section I

J.B. Li, H.X. Li, S.Q. Bi, Y. Sun, F. Gu, T.C. Yu. certify that they have NO affiliations with or involvement in any organization or entity with any financial interest (such as honoraria; educational grants; participation in speakers' bureaus; membership, employment, consultancies, stock ownership, or other equity interest; and expert testimony or patent-licensing arrangements), or non-financial interest (such as personal or professional relationships, affiliations, knowledge or beliefs) in the subject matter or materials discussed in this manuscript.

Declaration of competing interest

The authors declare no conflict of interests.

Acknowledgement

This study was supported by the National Natural Science Foundation of China (Grant No. 31970090).

Appendix A. Supplementary data

Supplementary data to this article can be found online at <https://doi.org/10.1016/j.jot.2023.10.006>.

References

- [1] Lew DP, Waldvogel FA. Osteomyelitis. *Lancet* 2004;364(9431):369–79.
- [2] Masters EA, Ricciardi BF, Bentley KLM, Moriarty TF, Schwarz EM, Muthukrishnan G. Skeletal infections: microbial pathogenesis, immunity and clinical management. *Nat Rev Microbiol* 2022;20(7):385–400.
- [3] Kremers HM, Nwojo ME, Ransom JE, Wood-Wentz CM, Melton 3rd LJ, Huddlestone 3rd PM. Trends in the epidemiology of osteomyelitis: a population-based study, 1969 to 2009. *J Bone Joint Surg Am* 2015;97(10):837–45.
- [4] Kavanagh N, Ryan EJ, Widaa A, Sexton G, Fennell J, O'Rourke S, et al. Staphylococcal osteomyelitis: disease progression, treatment challenges, and future directions. *Clin Microbiol Rev* 2018;31(2).
- [5] Yu Y, Tan L, Li Z, Liu X, Zheng Y, Feng X, et al. Single-atom catalysis for efficient sonodynamic therapy of methicillin-resistant *Staphylococcus aureus*-infected osteomyelitis. *ACS Nano* 2021;15(6):10628–39.
- [6] Tuchscher L, Medina E, Hussain M, Volker W, Heitmann V, Niemann S, et al. *Staphylococcus aureus* phenotype switching: an effective bacterial strategy to escape host immune response and establish a chronic infection. *EMBO Mol Med* 2011;3(3):129–41.
- [7] Valour F, Trouillet-Assant S, Riffard N, Tasse J, Flammier S, Rasigade JP, et al. Antimicrobial activity against intraosteoblastic *Staphylococcus aureus*. *Antimicrob Agents Chemother* 2015;59(4):2029–36.
- [8] Carryn S, Chanteux H, Seral C, Mingeot-Leclercq MP, Van Bambeke F, Tulkens PM. Intracellular pharmacodynamics of antibiotics. *Infect Dis Clin* 2003;17(3):615–34.
- [9] Renard C, Vanderhaeghe HJ, Claes PJ, Zenebergh A, Tulkens PM. Influence of conversion of penicillin G into a basic derivative on its accumulation and subcellular localization in cultured macrophages. *Antimicrob Agents Chemother* 1987;31(3):410–6.
- [10] Tulkens PM. Intracellular distribution and activity of antibiotics. *Eur J Clin Microbiol Infect Dis* 1991;10(2):100–6.
- [11] al-Nawas B, Shah PM. Intracellular activity of vancomycin and Ly333328, a new semisynthetic glycopeptide, against methicillin-resistant *Staphylococcus aureus*. *Infection* 1998;26(3):165–7.
- [12] Fraunholz M, Sinha B. Intracellular *Staphylococcus aureus*: live-in and let die. *Front Cell Infect Microbiol* 2012;2:43.
- [13] Josse J, Velard F, Gangloff SC. *Staphylococcus aureus* vs. Osteoblast: relationship and consequences in osteomyelitis. *Front Cell Infect Microbiol* 2015;5:85.
- [14] Alexander EH, Bento JL, Hughes Jr FM, Marriott I, Hudson MC, Bost KL. *Staphylococcus aureus* and *Salmonella enterica* serovar Dublin induce tumor necrosis factor-related apoptosis-inducing ligand expression by normal mouse and human osteoblasts. *Infect Immun* 2001;69(3):1581–6.
- [15] Zhou K, Li C, Chen D, Pan Y, Tao Y, Qu W, et al. A review on nanosystems as an effective approach against infections of *Staphylococcus aureus*. *Int J Nanomed* 2018;13:7333–47.
- [16] Noore J, Noore A, Li B. Cationic antimicrobial peptide LL-37 is effective against both extra- and intracellular *Staphylococcus aureus*. *Antimicrob Agents Chemother* 2013;57(3):1283–90.
- [17] Kaur S, Harjai K, Chhibber S. Bacteriophage-aided intracellular killing of engulfed methicillin-resistant *Staphylococcus aureus* (MRSA) by murine macrophages. *Appl Microbiol Biotechnol* 2014;98(10):4653–61.
- [18] Turk C, Petrik A, Sarica K, Seitz C, Skolarikos A, Straub M, et al. EAU guidelines on interventional treatment for urolithiasis. *Eur Urol* 2016;69(3):475–82.
- [19] Chaussy C, Brendel W, Schmiedt E. Extracorporeally induced destruction of kidney stones by shock waves. *Lancet* 1980;2(8207):1265–8.
- [20] Cheng JH, Wang CJ. Biological mechanism of shockwave in bone. *Int J Surg* 2015;24(Pt B):143–6.
- [21] Moya D, Ramon S, Schaden W, Wang CJ, Guiloff L, Cheng JH. The role of extracorporeal shockwave treatment in musculoskeletal disorders. *J Bone Joint Surg Am* 2018;100(3):251–63.
- [22] Schroeder AN, Tenforde AS, Jelsing EJ. Extracorporeal shockwave therapy in the management of sports medicine injuries. *Curr Sports Med Rep* 2021;20(6):298–305.
- [23] d'Agostino MC, Craig K, Tibalt E, Respizzi S. Shock wave as biological therapeutic tool: from mechanical stimulation to recovery and healing, through mechanotransduction. *Int J Surg* 2015;24(Pt B):147–53.
- [24] Prat F, Sibille A, Luccioni C, Pansu D, Chapelon JY, Beaumatin J, et al. Increased chemocytotoxicity to colon cancer cells by shock wave-induced cavitation. *Gastroenterology* 1994;106(4):937–44.
- [25] Gambihler S, Delius M. In vitro interaction of lithotripter shock waves and cytotoxic drugs. *Br J Cancer* 1992;66(1):69–73.
- [26] Hamza T, Li B. Differential responses of osteoblasts and macrophages upon *Staphylococcus aureus* infection. *BMC Microbiol* 2014;14:207.

- [27] Pumerantz A, Muppidi K, Agnihotri S, Guerra C, Venketaraman V, Wang J, et al. Preparation of liposomal vancomycin and intracellular killing of methicillin-resistant *Staphylococcus aureus* (MRSA). *Int J Antimicrob Agents* 2011;37(2):140–4.
- [28] Petty W, Spanier S, Shuster JJ, Silverthorne C. The influence of skeletal implants on incidence of infection. Experiments in a canine model. *J Bone Joint Surg Am* 1985;67(8):1236–44.
- [29] Rissing JP, Buxton TB, Weinstein RS, Shockley RK. Model of experimental chronic osteomyelitis in rats. *Infect Immun* 1985;47(3):581–6.
- [30] Smeltzer MS, Thomas JR, Hickmon SG, Skinner RA, Nelson CL, Griffith D, et al. Characterization of a rabbit model of staphylococcal osteomyelitis. *J Orthop Res* 1997;15(3):414–21.
- [31] Kodama T, Hamblin MR, Doukas AG. Cytoplasmic molecular delivery with shock waves: importance of impulse. *Biophys J* 2000;79(4):1821–32.
- [32] Tschoep K, Hartmann G, Jox R, Thompson S, Eigler A, Krug A, et al. Shock waves: a novel method for cytoplasmic delivery of antisense oligonucleotides. *J Mol Med (Berl)* 2001;79(5–6):306–13.
- [33] Zhang Y, Cheng H, Li W, Wu H, Yang Y. Highly-expressed P2X7 receptor promotes growth and metastasis of human HOS/MNNG osteosarcoma cells via PI3K/Akt/GSK3beta/beta-catenin and mTOR/HIF1alpha/VEGF signaling. *Int J Cancer* 2019;145(4):1068–82.
- [34] Grol MW, Panupinthu N, Korcok J, Sims SM, Dixon SJ. Expression, signaling, and function of P2X7 receptors in bone. *Purinergic Signal* 2009;5(2):205–21.
- [35] Gartland A, Hipskind RA, Gallagher JA, Bowler WB. Expression of a P2X7 receptor by a subpopulation of human osteoblasts. *J Bone Miner Res* 2001;16(5):846–56.
- [36] Surprenant A, Rassendren F, Kawashima E, North RA, Buell G. The cytolytic P2Z receptor for extracellular ATP identified as a P2X receptor (P2X7). *Science* 1996;272(5262):735–8.
- [37] Pelegrin P, Surprenant A. Pannexin-1 mediates large pore formation and interleukin-1beta release by the ATP-gated P2X7 receptor. *EMBO J* 2006;25(21):5071–82.
- [38] Sun D, Junger WG, Yuan C, Zhang W, Bao Y, Qin D, et al. Shockwaves induce osteogenic differentiation of human mesenchymal stem cells through ATP release and activation of P2X7 receptors. *Stem Cell* 2013;31(6):1170–80.
- [39] North RA. Molecular physiology of P2X receptors. *Physiol Rev* 2002;82(4):1013–67.
- [40] Abbracchio MP, Burnstock G, Verkhratsky A, Zimmermann H. Purinergic signalling in the nervous system: an overview. *Trends Neurosci* 2009;32(1):19–29.
- [41] Ren W, Rubini P, Tang Y, Engel T, Illes P. Inherent P2X7 receptors regulate macrophage functions during inflammatory diseases. *Int J Mol Sci* 2021;23(1).
- [42] Spellberg B, Lipsky BA. Systemic antibiotic therapy for chronic osteomyelitis in adults. *Clin Infect Dis* 2012;54(3):393–407.
- [43] Li Y, Liu L, Wan P, Zhai Z, Mao Z, Ouyang Z, et al. Biodegradable Mg-Cu alloy implants with antibacterial activity for the treatment of osteomyelitis: in vitro and in vivo evaluations. *Biomaterials* 2016;106:250–63.
- [44] Li J, Wang J, Wang D, Guo G, Yeung KWK, Zhang X, et al. Band gap engineering of titania film through cobalt regulation for oxidative damage of bacterial respiration and viability. *ACS Appl Mater Interfaces* 2017;9(33):27475–90.
- [45] Zhou S, Huang G, Chen G. Synthesis and biological activities of drugs for the treatment of osteoporosis. *Eur J Med Chem* 2020;197:112313.
- [46] Xu XY, He XT, Wang J, Li X, Xia Y, Tan YZ, et al. Role of the P2X7 receptor in inflammation-mediated changes in the osteogenesis of periodontal ligament stem cells. *Cell Death Dis* 2019;10(1):20.